

# Large-scale atmospheric circulation biases and changes in global climate model simulations and their importance for regional climate scenarios: a case study for West-Central Europe

A. P. van Ulden and G. J. van Oldenborgh

Koninklijk Nederlands Meteorologisch Instituut (KNMI), PO Box 201, 3730 AE, De Bilt, Netherlands

Received: 1 June 2005 – Accepted: 24 June 2005 – Published: 25 August 2005

Correspondence to: A. P. van Ulden (aad.van.uldens@knmi.nl)

© 2005 Author(s). This work is licensed under a Creative Commons License.

## Circulation biases and changes in global climate models

A. P. van Ulden and  
G. J. van Oldenborgh

Title Page

Abstract

Introduction

Conclusions

References

Tables

Figures

◀

▶

◀

▶

Back

Close

Full Screen / Esc

Print Version

Interactive Discussion

## Abstract

The credibility of regional climate change predictions for the 21st century depends on the ability of climate models to simulate global and regional circulations in a realistic manner. To investigate this issue, a large set of global coupled climate model experiments prepared for the Fourth Assessment Report of the Intergovernmental Panel on Climate Change has been studied. First we compared 20th century model simulations of longterm mean monthly sea level pressure patterns with ERA-40. We found a wide range in performance. Many models performed well on a global scale. For northern midlatitudes and Europe many models showed large errors, while other models simulated realistic pressure fields.

Next we focused on the monthly mean climate of West-Central Europe in the 20th century. In this region the climate depends strongly on the circulation. Westerlies bring temperate weather from the Atlantic Ocean, while easterlies bring cold spells in winter and hot weather in summer. In order to be credible for this region, a climate model has to show realistic circulation statistics in the current climate, and a response of temperature and precipitation variations to circulation variations that agrees with observations. We found that even models with a realistic mean pressure pattern over Europe still showed pronounced deviations from the observed circulation distributions. In particular, the frequency distributions of the strength of westerlies appears to be difficult to simulate well. This contributes substantially to biases in simulated temperatures and precipitation, which have to be accounted for when comparing model simulations with observations.

Finally we considered changes in climate simulations between the end of the 20th century and the end of the 21st century. Here we found that changes in simulated circulation statistics play an important role in climate scenarios. For temperature, the warm extremes in summer and cold extremes in winter are most sensitive to changes in circulation, because these extremes depend strongly on the simulated frequency of easterly flow. For precipitation, we found that circulation changes have a substantial

### Circulation biases and changes in global climate models

A. P. van Ulden and  
G. J. van Oldenborgh

Title Page

Abstract

Introduction

Conclusions

References

Tables

Figures

◀

▶

◀

▶

Back

Close

Full Screen / Esc

Print Version

Interactive Discussion

influence, both on mean changes and on changes in the probability of wet extremes and of long dry spells. Because we do not know how reliable climate models are in their predictions of circulation changes, climate change predictions for Europe are as yet uncertain in many aspects.

## 1. Introduction

Global coupled climate models are indispensable tools in climate analysis. Such models are credible if they are able to produce realistic simulations of large scale patterns of the atmospheric circulation and of other climate variables. An assessment of the performance of global coupled models can be found in the Third Assessment Report of IPCC (IPCC 2001), and in Achuta Rao et al. (2004). Recently many new coupled model simulations have been made, both for the 20th century climate and for various future emission scenarios. Model output has been made accessible for analysis by external groups, in preparation for the Fourth Assessment Report of IPCC (see Acknowledgements and Table 1). This has created a unique opportunity to compare simulations by many different models with observations, and to compare climate change projections by these models.

This paper deals primarily with the monthly mean climate in West-Central Europe. In this region the climate depends strongly on the atmospheric circulation. Westerlies carry maritime air from the Atlantic Ocean to the continent, while easterlies bring cold weather in winter and hot weather in summer. In order to be credible for this region, a climate model has to show realistic circulation statistics in the current climate. A first requirement is that a model is able to simulate the mean circulation over the globe and over Europe in a realistic manner. Biases in the mean circulation are indications for important model deficiencies, such as a poor representation of the frequency of atmospheric blockings (D'Andrea et al., 1998) or less credible thermohaline circulations (Thorpe, 2005). Therefore, we start our analysis with a comparison of model simulations of longterm mean monthly sea level pressure patterns with global and regional

### Circulation biases and changes in global climate models

A. P. van Ulden and  
G. J. van Oldenborgh

Title Page

Abstract

Introduction

Conclusions

References

Tables

Figures

◀

▶

◀

▶

Back

Close

Full Screen / Esc

Print Version

Interactive Discussion

---

**Circulation biases  
and changes in  
global climate  
models**

---

A. P. van Ulden and  
G. J. van Oldenborgh

---

[Title Page](#)[Abstract](#)[Introduction](#)[Conclusions](#)[References](#)[Tables](#)[Figures](#)[◀](#)[▶](#)[◀](#)[▶](#)[Back](#)[Close](#)[Full Screen / Esc](#)[Print Version](#)[Interactive Discussion](#)

observations. This comparison is presented in Sect. 2. Based on this test we selected a sub-set of models which show relatively realistic mean pressure patterns over the globe and over Europe for further analysis of the climate in West-Central Europe.

For the description of regional circulation statistics, we use three geostrophic flow indices: the two components of the geostrophic wind and the geostrophic vorticity. Variations in such flow indices have been shown to correlate well with variations in monthly mean temperatures and precipitation (Turnpenny et al., 2002; Van Oldenborgh and van Ulden, 2003; Van Ulden et al., 2005). In Sect. 3 we compare 20th century model simulations of these flow indices with observations in West-Central Europe. In addition we will compare observed relations between circulation on the one hand, and temperature and precipitation on the other hand with the corresponding relations in the model simulations. This serves as a further test on the internal consistency of the model simulations. This analysis provides also an estimate of the contribution of biases in simulated circulations to biases in mean temperature and mean precipitation.

In Sect. 4 we analyse simulated changes in the atmospheric circulation, primarily for the SRES A2 emission scenario. Using the techniques developed in Sect. 3, we will estimate the contribution of mean circulation changes to changes in temperature and precipitation. This is an important issue in the development of regional climate change scenarios, as has been shown by Jylhä et al. (2004). Further, we will explore the influence of changes in the circulation statistics on changes in the distributions of monthly mean temperature and precipitation.

We conclude this paper with a discussion on the complex role of atmospheric circulation statistics in regional climate simulations (Sect. 5).

## 2. Global and regional patterns of longterm mean sea level pressure

In this section we analyse longterm averages of monthly sea level pressure patterns. For the validation of simulated sea level pressure patterns we use data from ERA-40 (Kållberg et al., 2004). In a recent paper Bromwich and Fogt (2004) found that ERA-40

---

**Circulation biases  
and changes in  
global climate  
models**

A. P. van Ulden and  
G. J. van Oldenborgh

---

[Title Page](#)[Abstract](#)[Introduction](#)[Conclusions](#)[References](#)[Tables](#)[Figures](#)[◀](#)[▶](#)[◀](#)[▶](#)[Back](#)[Close](#)[Full Screen / Esc](#)[Print Version](#)[Interactive Discussion](#)

is not well constrained by observations in data-sparse regions of the Southern Hemisphere during the presatellite era. Therefore we used ERA-40 data starting from 1973. The average pressure patterns before 1973 are however very similar to the average patterns thereafter. This is probably due to a realistic climatological behaviour of the ERA-40 model. Using ERA-40 data has the added advantage, that ERA-40 deals with orography in a similar manner as climate models do. Thus, there is no reason to exclude mountainous regions from the comparison. For the validation over Europe we used the ADVICE pressure reconstruction by Jones et al. (1999), which is directly based on observations in the period 1780–1995. From the model simulations we used the average of all available members of the 20th century runs. For each month these ensemble mean patterns were compared with observations for the globe, for the tropics (30° S–30° N), for southern latitudes (30° S–90° S), for northern latitudes (30° N–90° N) and for Europe (30° W–40° E, 35° N–65° N). The European domain includes Iceland and the Azores and thus comprises an important part of the North Atlantic (see Fig. 2).

In Fig. 1 we present the spatial standard deviations of the difference fields between simulated and observed pressure patterns for Europe. We see a wide range in model performance. In order to judge the quality of the models it is useful to look at the explained spatial variance, which is defined as:

$$VAR_{expl} = 1 - VAR_{diff} / VAR_{obs}. \quad (1)$$

If for a given model the standard deviation of the difference field is larger than the standard deviation of the observed field, the explained variance is negative for that model. In Table 2, we show the annual rms-values of the 12 monthly spatial standard deviations and the annual averages of the explained variance for each month. We see that for the tropics all models explain more than 50% of the spatial variance. For southern latitudes 6 models have a poor performance. This is due to unrealistic pressure fields over Antarctica. The pressure fields for northern latitudes appear to be most difficult to simulate. Only 5 models explain more than 50% of the spatial variance. Important bias regions are the North Atlantic and the Asian continent. Many models have a poor performance over Europe as well.

---

**Circulation biases  
and changes in  
global climate  
models**

A. P. van Ulden and  
G. J. van Oldenborgh

---

[Title Page](#)[Abstract](#)[Introduction](#)[Conclusions](#)[References](#)[Tables](#)[Figures](#)[◀](#)[▶](#)[◀](#)[▶](#)[Back](#)[Close](#)[Full Screen / Esc](#)[Print Version](#)[Interactive Discussion](#)

Except for Europe, the above comparison is based on a rather short observation record, so it is possible that natural variability plays a role in this comparison. Unfortunately we have no reliable long observation records for the global pressure fields. For Europe, however we can use the long observation record to study natural variability. It appears that individual 30 y mean fields differ less than 1 hPa from the longterm mean field (Fig. 1). Also the difference between ERA-40 and the long analysed record is less than 1 hPa for all months (Fig. 1). This indicates that a 30 y year averaging period is sufficient to remove most of the natural variability in the European pressure patterns, and that differences caused by different analysis methods are smaller than the systematic errors in global model simulations.

Another important issue concerns the spatial scales of the longterm mean bias patterns. It appears that the dominant scales are very large: i.e. thousands of kilometers. This is important for climate simulations by high resolution regional models which have to use boundary conditions from global models. If the global model has a large-scale bias, it is likely that the regional model will inherit much of this bias (Van Ulden et al., 2005).

### 3. The 20th-century climate in West-Central Europe

#### 3.1. Matching scales, selection of observations and selection of models

Our test domain in West-Central Europe is shown in Fig. 2. The domain is situated north of the Alps. The climate is under the influence of prevailing westerlies and moderately maritime. The geostrophic flow indices were computed in the area  $0^{\circ}$ – $20^{\circ}$  E,  $45^{\circ}$ – $55^{\circ}$  N. The geostrophic wind was computed from the sea level pressures at the four corners of the domain, using a fixed value for the air density ( $1.2 \text{ kg m}^{-3}$ ). For the geostrophic vorticity we used the difference between the mean pressure at the four corners of the domain and the pressure in the center as a simple proxy. The locations of the centre of the domain and of its four corners are away from major orography, thus

---

**Circulation biases  
and changes in  
global climate  
models**

---

A. P. van Ulden and  
G. J. van Oldenborgh

---

[Title Page](#)[Abstract](#)[Introduction](#)[Conclusions](#)[References](#)[Tables](#)[Figures](#)[◀](#)[▶](#)[◀](#)[▶](#)[Back](#)[Close](#)[Full Screen / Esc](#)[Print Version](#)[Interactive Discussion](#)

5 details of procedures for the reduction of surface pressure do not play an important role. The ADVICE pressure analysis (Jones et al., 1999) was used as observation. Since this analysis has a  $5^\circ$  lat  $\times$   $10^\circ$  lon resolution, the pressure fields simulated by the climate models were smoothed to match this resolution. We tested the smoothing procedure by comparing the smoothed ERA-40 fields with the ADVICE fields and found an excellent agreement, both with respect to the mean indices and with respect to their variability. Thus we used smoothed ERA-40 data to extend the ADVICE analysis to the year 2000.

10 For temperature and precipitation we used the region  $6^\circ$ – $14^\circ$  E,  $48.5^\circ$ – $53.5^\circ$  N as test domain. This land domain includes a major part of Germany and smaller parts of adjacent countries. The domain is at a suitable distance from the Alps and is characterised by flat plains and modest orography. Model output was averaged over this domain. This removes the direct impact of differences in model resolution, which ranges from about 120 km to 440 km in West-Central Europe.

15 Temperature observations for the full 20th century were taken from the updated  $0.5^\circ$  gridded data set by New et al. (1999; 2000). We compared the temperatures in this data set with ERA-40 for the ERA-40 period and found an excellent agreement.

20 Precipitation data were also taken from New et al. (1999, 2000). This data set was not corrected for undercatchment due to snow and wind. In order to obtain an estimate of this undercatchment, we compared the New et al. (2000) data with a detailed calibrated precipitation data set for the German part of the river Rhine basin (Van den Hurk et al., 2005). This data set covers most of the western half of our test region and is available for 1961–1995. In the overlapping domain and overlapping time period, the monthly mean precipitations of the two data sets were highly correlated ( $r=0.95$ ). The comparison indicated a significant undercatchment in the New et al. data set, ranging from about 2% in summer months to 20% in winter months. We corrected the New et al. (2000) data using this estimate of undercatchment in our full test domain.

25 For the model validation given hereafter, we selected the 8 models with the highest skill for the simulated sea level pressure fields in the European domain, as given in

Table 2. For comparison, we have also included 2 models with a poor performance. We included only the first ensemble member of each 20th-century model simulation in our analysis.

### 3.2. Geostrophic flow statistics in the 20th century

5 In Fig. 3 we show the mean and the standard deviation of the west-component of the geostrophic wind for each month of the year. Most models have a mean westerly bias in winter, which is quite extreme for CCSM3. This positive bias is caused by a deeper than observed Icelandic low and a positive pressure bias over the Mediterranean. In summer most models have a negative (i.e. easterly) bias in G-west. GISSer even has  
10 a pronounced mean easterly flow in summer. This negative bias is caused by a high pressure bias over Northern Europe and a low pressure bias over the Mediterranean. The standard deviations are relatively well modelled. The importance of biases in G-west can be further illustrated by looking at the frequency distributions.

In Fig. 4a we show the cumulative frequency distributions for  $G_W$  in January. Winter months with a mean flow from the east are characterised by cold and dry continental weather. Thus the frequency of such months is an important ingredient of the winter climate. We see that GISSer overpredicts this frequency. HadGEM has a pronounced westerly bias in January, but still has a significant overlap with the observed distribution. The westerly bias in the CCSM3 simulation is very large, and the simulated distribution  
20 has little overlap with the observed distribution.

In Fig. 4b we show the cumulative frequency distributions for  $G_W$  in July. Summer months with a mean easterly flow have predominantly warm and dry weather. About 10% of the observed July months have a mean flow from the east. Most models simulate a much higher percentage. For GISSer all months have a mean flow from the east.  
25 On the other hand, ECHAM5 has a weak westerly bias in summer.

The model simulations of the south component of the geostrophic wind are relatively close to the observations and to each other, as is shown in Fig. 5.

In Fig. 6 we show the comparison for the geostrophic vorticity. Many models simu-

---

## Circulation biases and changes in global climate models

A. P. van Ulden and  
G. J. van Oldenborgh

---

Title Page

Abstract

Introduction

Conclusions

References

Tables

Figures

◀

▶

◀

▶

Back

Close

Full Screen / Esc

Print Version

Interactive Discussion

late a higher than observed mean geostrophic vorticity, and in summer a higher than observed standard deviation. In Fig. 7 the cumulative frequency distributions for January and July are given. GISSer deviates most from the observations, in particular in July. The distribution for July simulated by this model has no overlap with the observed distribution.

These results show that biases in the simulated geostrophic flow indices are quite large, even for models which produce relatively realistic pressure fields over Europe. We may expect that these biases have an impact on simulations of temperature and precipitation. In the next sections we will investigate the importance of these impacts.

### 3.3. Relations between circulation variations and temperature variations

Interannual variability of the atmospheric circulation is a prime source for variability in monthly mean temperature and precipitation (Turnpenny et al., 2002; Van Oldenborgh and van Ulden, 2003). Relations between circulation on the one hand, and temperature and precipitation on the other hand, can be used to analyse the influence of differences in circulation statistics on mean temperatures and precipitation, and on their variability.

For the description of the influence of the circulation on temperature, we use a simple linear model. Monthly Circulation Temperature Anomalies are defined as:

$$CTA = A_S \Delta G_S + A_W \Delta G_W + A_V \Delta G_V + M \quad (2)$$

where  $\Delta G_S$ ,  $\Delta G_W$  and  $\Delta G_V$  are circulation anomalies relative to the mean observed values for the 20th century and where  $M$  is a memory term for past circulations. This term is modeled as an exponentially decaying memory with  $\tau$  as e-folding period. We retained the memory for the circulation in the previous 3 months. Monthly values of the numerical coefficients  $A_S$ ,  $A_W$ ,  $A_V$  and the memory  $\tau$  were obtained from a least-square fit for the observations of the 20th century. We then multiplied the numerical coefficients by a scaling factor, such that the monthly CTA had the same variance as the observed temperatures. Thus CTA is a variance conserving regression to the observations.

## Circulation biases and changes in global climate models

A. P. van Ulden and  
G. J. van Oldenborgh

Title Page

Abstract

Introduction

Conclusions

References

Tables

Figures

◀

▶

◀

▶

Back

Close

Full Screen / Esc

Print Version

Interactive Discussion

## Circulation biases and changes in global climate models

A. P. van Ulden and  
G. J. van Oldenborgh

Title Page

Abstract

Introduction

Conclusions

References

Tables

Figures

◀

▶

◀

▶

Back

Close

Full Screen / Esc

Print Version

Interactive Discussion

This simple model performs quite well, with correlations around 0.8 (see Fig. 9). In winter and summer  $G_W$  is the dominating term in Eq. (2). In the transition months  $G_S$  and  $G_V$  give the largest contribution to the explained variance. The memory length varies typically between 0.3 m and 0.9 m. The contribution of the memory term to the explained variance is significant in late winter (memory for snow feedback) and in late summer (memory for soil moisture depletion). Nearby seas produce memory effects all year round.

For the models the circulation anomalies are computed from modeled values of  $\Delta G_S$ ,  $\Delta G_W$ , and  $\Delta G_V$  using Eq. (2) and the observed values of  $A_S$ ,  $A_W$ ,  $A_V$ , and the memory  $\tau$ . The variance conserving regression line for simulated temperature anomalies is given by:

$$TA_{Regr.} = \langle TA \rangle + S_T CTA - \langle CTA \rangle. \quad (3)$$

Where  $\langle TA \rangle$  is the mean simulated temperature anomaly and  $S_T$  the slope that is given by

$$S_T = A_{TA} / A_{CTA}, \quad (4)$$

where  $A_{TA}$  denotes the standard deviation of the modeled temperature anomalies  $TA$  and  $A_{CTA}$  the standard deviation of the modeled  $CTA$ . The mean temperature bias due to the bias in the simulated circulations is given by

$$TA_{CircBias} = S_T \langle CTA \rangle. \quad (5)$$

The analysis procedure described by Eqs. (2)–(5) is illustrated in Fig. 8, which shows scatter plots, means and regression lines of simulated and observed temperature anomalies against circulation temperature anomalies.

Next we analyse the performance of 10 models. In Fig. 9a we show the monthly correlations. In winter all models show high correlations, similar to the observed correlations. In summer some models show markedly lower than observed correlations. In general the correlations are satisfactory, indicating that models produce temperature

## Circulation biases and changes in global climate models

A. P. van Ulden and  
G. J. van Oldenborgh

Title Page

Abstract

Introduction

Conclusions

References

Tables

Figures

◀

▶

◀

▶

Back

Close

Full Screen / Esc

Print Version

Interactive Discussion

variations in a similar manner as the real climate. In Fig. 9b, we show the slope of the regression lines. These are reasonably close to unity. There seems to be a tendency that models with a westerly circulation bias simulate lower slopes than models with an easterly bias. This is consistent with the idea that a westerly circulation bias leads to a more maritime climate, which is less variable, while an easterly bias produces a more continental and more variable climate. Thus a mean bias in the circulation may have a profound influence on the variability of the monthly mean temperatures.

Next we look at biases in the mean temperature. In Fig. 10 we show the total temperature bias in the 20th-century model simulations, the temperature bias attributable to circulation biases and the residual temperature bias, which is obtained by subtracting the circulation induced bias from the total bias. We see a wide range in biases. The circulation induced biases are largest for GISSer and CCSM3. This is understandable, because these models have the strongest circulation biases. CCC3.1 has the largest residual bias in particular in March–April. This pronounced cold bias can be partly explained by a pronounced cold bias in the Northern Hemisphere temperatures simulated by this model. Also GFDL2.1 has a cold Northern Hemisphere bias. These results show that an analysis of regional circulation statistics should be an integral part of the validation of regional model performance, since circulation induced biases can be of the same order as other biases. A much more detailed analysis would be needed to understand all the biases, but this falls outside the scope of this paper.

### 3.4. Relations between circulation variations and precipitation variations

The analysis for precipitation is very similar to that for temperature. Circulation Precipitation Anomalies were defined as:

$$CPrA = B_S \Delta G_S + B_W \Delta G_W + B_V \Delta G_V + M. \quad (6)$$

This model performs quit well, with correlations around 0.7 for summer months and 0.8 for winter months (see Fig. 11).  $\Delta G_W$  is the most important contributor to the

explained variance for all months, but the geostrophic vorticity  $\Delta G_V$  is almost as important. We found no memory effects.

In Fig. 11a, we show the correlations between precipitation and circulation for the observations and for the model simulations. We see that, in general, the models have higher than observed correlations. Only GISSer shows low correlations in summer. Figure 11b shows the slope of the precipitation regression lines. In general this simulated slope is weaker than observed. This is partly caused by the higher than observed variability in the Geostrophic Vorticity that is simulated by the models (see Fig. 6b).

In Fig. 12 we show the precipitation biases for the 20th century simulations. These biases are given as a percentage of the monthly mean observed precipitation. We see that the biases are large. Noteworthy are the large circulation bias for CCSM3 in winter and the wet bias for GFDL2.1 and HadCM3 in summer. GISSer has a dry bias in many months. Again it is apparent that for a region like West-Central Europe it is useful to consider circulation statistics when validating simulated precipitation.

## 4. Climate change in West-Central Europe from the 20th century to 2071–2100

### 4.1. Mean changes

In the previous sections we have seen that only models with reasonable circulation statistics are credible enough for using them to analyse climate change. For HadGEM no scenario simulations were available at the time this analysis was made. This leaves 7 credible models for the analysis of climate change in West-Central Europe. For 6 models A2 scenario simulations were available, while for MIROCchi an A1B emission scenario was used.

In Fig. 13 we show the mean change in geostrophic flow indices from the 20th century to the scenario period 2071–2100. Although the models differ significantly in the extent of the simulated circulation changes, there is a general pattern in the changes. In winter there is a tendency towards more westerly and more anticyclonic circulations.

## Circulation biases and changes in global climate models

A. P. van Ulden and  
G. J. van Oldenborgh

Title Page

Abstract

Introduction

Conclusions

References

Tables

Figures

◀

▶

◀

▶

Back

Close

Full Screen / Esc

Print Version

Interactive Discussion

---

**Circulation biases  
and changes in  
global climate  
models**

A. P. van Ulden and  
G. J. van Oldenborgh

---

In late summer (July–September) there is a tendency towards more north-easterly and more anticyclonic flow. These simulated circulation changes resemble the trends in the atmospheric circulation that have been observed in the later part of the 20th century (Van Oldenborgh and van Ulden, 2003; Osborn, 2004). It is still unclear if this is a  
5 robust aspect of climate change due to greenhouse gas forcing.

Figure 14 shows total temperature changes, changes due to circulation changes and residual changes. Total changes (Fig. 14a) are highest in late summer (J, A, S), while winter months show a secondary maximum. This annual cycle in the temperature changes seems to be at least partly due to circulation changes, as is shown in  
10 Fig. 14b. August shows the largest range in circulation induced temperature changes: from almost no change for MIROC*hi* and MRI2.3.2 to more than 3 K for GFDL2.1.

The residual temperature changes in Fig. 14c also show a large range, but the changes are more evenly distributed over the year. In this figure the differences reflect, amongst other factors, the differences in global climate sensitivity between the  
15 models.

These results suggest that it may be feasible to construct climate change scenarios by decomposing temperature changes into a part that scales with changes in global mean temperature and a part that is related to changes in circulation. This idea has been explored by Van Oldenborgh and van Ulden (2003) for the observed climate in  
20 the Netherlands. Such a decomposition may be even more useful in the simulations of precipitation changes, which are shown in Fig. 15.

In Fig. 15a we see a very pronounced annual cycle in simulated precipitation changes for 5 of the 7 models. In the circulation induced precipitation changes this feature is even present for all models, although the amplitude of this annual cycle varies considerable between models. After removal of the circulation signal, a much  
25 more transparent residual signal results. For most months a modest increase in precipitation is shown. This increase is probably related to changes in the partitioning of the radiative flux convergence at the earth surface over the atmospheric latent and sensible heat fluxes and the heat flux into soil and water. This partitioning depends on

[Title Page](#)[Abstract](#)[Introduction](#)[Conclusions](#)[References](#)[Tables](#)[Figures](#)[◀](#)[▶](#)[◀](#)[▶](#)[Back](#)[Close](#)[Full Screen / Esc](#)[Print Version](#)[Interactive Discussion](#)

---

**Circulation biases  
and changes in  
global climate  
models**

---

A. P. van Ulden and  
G. J. van Oldenborgh

---

[Title Page](#)[Abstract](#)[Introduction](#)[Conclusions](#)[References](#)[Tables](#)[Figures](#)[◀](#)[▶](#)[◀](#)[▶](#)[Back](#)[Close](#)[Full Screen / Esc](#)[Print Version](#)[Interactive Discussion](#)

the temperature, at least over surfaces with sufficient moisture supply (Priestley and Taylor, 1972; Holtslag and van Ulden, 1983). All other things being equal, this theory predicts an increase in evaporation of about 2% per degree warming. The models that are analysed here produce a warming of about 3–4 K. Thus we would expect an increase in precipitation of about 7% in the absence of circulation changes. This is roughly consistent with the results shown in Fig. 15c.

In late summer (J, A, S) soil moisture depletion may play an important role in the hydrological budget. If the soil dries out the evaporation is reduced and simple relations between temperature and precipitation break down. If a model is insufficiently capable of conserving winter precipitation till late summer, the model may have a dry bias which becomes only apparent in late summer (Van den Hurk et al., 2005; Lenderink et al., 2005; Van Ulden et al., 2005). While severe summer drying does occur occasionally in West-Central Europe (for example in 2003), it may happen far more often in some models, while it does not in other models. This may explain the wide range of model results for late summer. We will return to this issue in the next section where we look at specific distributions for the 6 models which used an A2 scenario.

#### 4.2. Changes in distributions

In this section we use scatter plots of the type introduced in Fig. 8, for illustrating and discussing changes in distributions for 6 models. Each figure gives the regression line and the mean for the observations, while scatter plots, regression and means are given for the simulated periods 1971–2000 and 2071–2100. Because these periods cover only 30 y, we combine monthly values of December, January and February into one ensemble of 90 months to represent winter months distributions. In order to represent late summer distributions we combine July, August and September. We first discuss temperature and precipitation changes for winter months, which are shown in the Figs. 16 and 17.

In Fig. 16 we see that the slope of the regression line for temperature decreases in the scenario simulations. At higher temperatures the sensitivity of the temperature

---

**Circulation biases  
and changes in  
global climate  
models**A. P. van Ulden and  
G. J. van Oldenborgh

---

[Title Page](#)[Abstract](#)[Introduction](#)[Conclusions](#)[References](#)[Tables](#)[Figures](#)[◀](#)[▶](#)[◀](#)[▶](#)[Back](#)[Close](#)[Full Screen / Esc](#)[Print Version](#)[Interactive Discussion](#)

to circulation variations is reduced. This is caused by two factors. In the first place warmer temperatures reduce the impact of cold snow feed backs. In the second place the simulated shift to warmer circulations leads to a lower frequency of months with a cold snow feedback. Therefore, cold extremes are highly sensitive to changes in the atmospheric circulation.

Figure 17 gives the simulations for precipitation. Here we see a general increase in the variability in the scenario simulations. A certain increase in the slopes is to be expected, because a temperature increase will enhance all precipitation by a similar percentage, which automatically leads to a steeper slope.

In Fig. 18 we show the temperature simulations for late summer. We see that the models differ greatly in these summer simulations. MRI2.3.2 and CCC3.1 show hardly any change in the slope of the regression line. ECHAM5 and MIROChi show a modest increase in variability. HadCM3 and especially GFDL2.1 show a very pronounced increase in the slope of the regression line. For an interpretation of these results it is useful to look at the precipitation simulations as well. Figure 19 shows that HadCM3 and especially GFDL2.1 show the most pronounced changes towards dry circulations. This is primarily caused by an increase in the frequency of easterly continental flow. Therefore, the strong temperature response of these two models can be understood as follows. Enhanced frequencies of dry flows from the continent lead to an enhanced soil moisture depletion, to a reduction in evaporation and an enhancement of the sensible heat flux which produces strong warming. These interactions have a pronounced impact on the scaling of precipitation with temperature. While this scaling works well for westerly flow from the Atlantic Ocean, it breaks down for easterly flow in late summer. For easterly flow in late summer the reduction of evaporation may reverse the precipitation-temperature relation, as has been shown by Lenderink et al. (2005) in a detailed analysis of the variability of summer time temperatures. It is even possible that the atmospheric circulation in summer is affected by differential heating due to soil moisture depletion (Van Ulden et al., 2005).

The expected summer climate is therefore determined by a non-linear combination

of circulation changes, soil moisture depletion and possible dynamical feedbacks to the resulting heating. The coupled climate models differ wildly in the simulation of these factors. Apparently, the future summer climate is hard to predict.

## 5. Discussion

5 Many coupled climate models are able to simulate the long-term mean of monthly global patterns of the sea level pressure. Unfortunately, this is not the case for northern midlatitudes and for Europe. An important result of the present analysis is that bias patterns in sea level pressure fields simulated by global coupled models have very large scales of thousands of kilometers. This has consequences for the practice of regional climate modeling, which relies on boundary conditions produced by global models. If such models have large-scale errors in their simulations, it is likely that these errors are to a great extent imported by the nested regional models.

We analysed a subset of models that performed well for Europe in more detail. For these models the statistics of geostrophic flow indices were compared with observations. We found that models differed significantly in their simulation of the frequency distribution of the west component of the geostrophic wind. Apparently, models have difficulties in getting the frequency of blocking situations correct. This deficiency and other errors in simulated circulations have an important impact on simulated temperatures and precipitation. In particular, distributions of monthly mean temperature and precipitation are quite sensitive to biases and changes in the distribution of geostrophic flow indices.

Many models show changes in the simulated atmospheric circulations between the control runs and the scenario run. Simulations for winter months show in general a shift towards warmer and wetter circulations (stronger westerlies). Temperature variability is reduced, while the variability in precipitation increases in winter. Simulations for summer months show a shift towards warmer and drier circulations (stronger easterlies). Temperature and precipitation variability increase in future summers. The net

### Circulation biases and changes in global climate models

A. P. van Ulden and  
G. J. van Oldenborgh

Title Page

Abstract

Introduction

Conclusions

References

Tables

Figures

◀

▶

◀

▶

Back

Close

Full Screen / Esc

Print Version

Interactive Discussion

change in mean summer precipitation is unclear. Some models give a net precipitation increase, while other models simulate drier summers.

The simple model that we have used to describe relations between circulations on the one hand and temperature and precipitation on the other hand is useful to describe the climate in West-Central Europe for most months of the year at the present levels of uncertainty. In late summer, non-linear feedbacks involving soil moisture render its utility more limited. Still it serves to demonstrate that biases and changes in the atmospheric circulation deserve far more attention in model validation and in the development of climate change scenarios than these issues have received in the past.

*Acknowledgements.* We acknowledge the international modeling groups for providing their data for analysis, the Program for Climate Model Diagnosis and Intercomparison (PCMDI) for collecting and archiving the model data, the JSC/CLIVAR Working Group on Coupled Modelling (WGCM) and their Coupled Model Intercomparison Project (CMIP) and Climate Simulation Panel for organizing the model data analysis activity, and the IPCC WG1 TSU for technical support. The IPCC Data Archive at Lawrence Livermore National Laboratory is supported by the Office of Science, U.S. Department of Energy.

## References

- Achuta Rao, K., Covey, C., Doutriaux, C., Fionino, M., Gleckler, P., Philips, T., Sperber, K., and Taylor, K.: An Appraisal of Coupled Climate Model Simulations, edited by: Bader, D., University of California, Lawrence Livermore National Laboratory, UCRL-TR-202550, 197, 2004.
- Bromwich, D. H. and Fogt, R. L.: Strong trends in the skill of the ERA-40 and NCEP-NCAR reanalyses in the high and midlatitudes of the Southern Hemisphere, *J. Climate*, 17, 4603–4619, 2004.
- D'Andrea, F., Tibaldi, S., Blackburn, M., Boer, G., Déqué, M., Dugas, B., Ferranti, L., Hunt, B., Kitho, A., Randall, D., Roeckner, E., Rowell, D., Straus, D., Sato, N., van den Dool, H. and Williamson, D.: Northern Hemisphere atmospheric blocking as simulated by 15 atmospheric general circulation models in the period 1979–1988, *Clim. Dyn.*, 14, 385–407, 1998.

## Circulation biases and changes in global climate models

A. P. van Ulden and  
G. J. van Oldenborgh

Title Page

Abstract

Introduction

Conclusions

References

Tables

Figures

◀

▶

◀

▶

Back

Close

Full Screen / Esc

Print Version

Interactive Discussion

---

**Circulation biases  
and changes in  
global climate  
models**A. P. van Ulden and  
G. J. van Oldenborgh

---

Title Page

Abstract

Introduction

Conclusions

References

Tables

Figures

◀

▶

◀

▶

Back

Close

Full Screen / Esc

Print Version

Interactive Discussion

Delworth, T. L., Broccoli, A. J., Rosati, A., Stouffer, R. J., Balaji, V., Beesley, J. A., Cooke, W. F., Dixon, K. W., Dunne, J., Dunne, K. A., Durachta, J. W., Findell, K. L., Ginoux, P., Gnanadesikan, A., Gordon, C. T., Griffies, S. M., Gudgel, R., Harrison, M. J., Held, I. M., Hemler, R. S., Horowitz, L. W., Klein, S. A., Knutson, T. R., Kushner, P. J., Langenhorst, A. R., Lee, H. C., Lin, S. J., Lu, J., Malyshev, S. L., Milly, P. C. D., Ramaswamy, V., Russell, J., Schwarzkopf, M. D., Shevliakova, E., Sirutis, J. J., Spelman, M. J., Stern, W. F., Winton, M., Wittenberg, A. T., Wyman, B., Zeng, F., and Zhang, R.: GFDL's CM2 global coupled climate models – Part 1: formulation and simulation characteristics, *J. Climate*, accepted, 2005.

Gordon, C., Cooper, C., Senior, C. A., Banks, H., Gregory, J. M., Johns, T. C., J. F. B. Mitchell, J. F. B., and R. Wood, R. A.: The simulation of SST, sea ice extents and ocean heat transport in a version of the Hadley Centre coupled model without flux adjustments, *Climate Dyn.*, 16, 147–168, 2000.

Gordon, H. B., Rotstajn, L. D., McGregor, J. L., Dix, M. R., Kowalczyk, E. A., O'Farrell, S. P., Waterman, L. J., Hirst, A. C., Wilson, S. G., Collier, M. A., Watterson, I. G., and Elliott, T. I.: The CSIRO Mk3 climate system model, Technical Report 60, CSIRO Atmospheric Research, Aspendale, [www.dar.csiro.au/publications/gordon\\_2002a.pdf](http://www.dar.csiro.au/publications/gordon_2002a.pdf), 2002.

Holtstlag, A. A. M., and van Ulden, A. P.: A simple scheme for daytime estimates of the surface fluxes from routine weather data, *J. Climate Appl. Meteor.*, 22, 517–529, 1983.

IPCC 2001: Climate Change 2001: The Scientific Basis, Contribution of Working Group I to the Third Assessment Report of the Intergovernmental Panel on Climate Change, Cambridge University Press, 881, 2001.

Johns, T., Durman, C., Banks, H., Roberts, M., McLaren, A., Ridley, J., Senior, C., Williams, K., Jones, A., Keen, A., Rickard, G., Cusack, S., Joshi, M., Ringer, M., Dong, B., Spencer, H., Hill, R., Gregory, J., Pardaens, A., Lowe, J., Bodas-Salcedo, A., Start, S., and Searl, Y.: HadGEM1 model description and analysis of preliminary experiments for the IPCC Fourth Assessment Report, Technical Report 55, U.K. Met Office, Exeter, U.K., [www.metoffice.gov.uk/research/hadleycentre/pubs/HCTN/index.html](http://www.metoffice.gov.uk/research/hadleycentre/pubs/HCTN/index.html), 2004.

Jones, P. D., Davies, T. D., Lister, D. H., Slonosky, V., Jonsson, T., Barring, L., Jonsson, P., Maheras, P., Kolyva-Machera, F., Barriendos, M., Martin-Vide, J., Rodriguez, R., Alcoforado, M. J., Wanner, H., Pfister, C., Luterbacher, J., Rickli, R., Schuepbach, E., Kaas, E., Schmith, T., Jacobeit, J., and Beck, C.: Monthly mean pressure reconstructions for Europe for the 1780–1995 period, *Int. J. Climatol.*, 19, 347–364, 1999.

Jylhä, K., Tuomenvirta H., and Ruosteenoja, K.: Climate change projections for Finland during

---

**Circulation biases  
and changes in  
global climate  
models**

---

A. P. van Ulden and  
G. J. van Oldenborgh

---

Title Page

Abstract

Introduction

Conclusions

References

Tables

Figures

◀

▶

◀

▶

Back

Close

Full Screen / Esc

Print Version

Interactive Discussion

the 21st century, *Boreal Env. Res.*, 9, 127–152, 2004.

K-1 Model Developers: K-1 coupled model (MIROC) description, Technical Report 1, Center for Climate System Research, University of Tokyo, <http://www.ccsr.u-tokyo.ac.jp/kyosei/hasumi/MIROC/tech-repo.pdf>, 2004.

5 Kim, S.-J., Flato, G. M., de Boer, G. J., and McFarlane, N. A.: A coupled climate model simulation of the last glacial maximum, part 1: transient multi-decadal response, *Climate Dyn.*, 19, 515–537, 2002.

Källberg, P., Simmons, A., Uppala S., and Fuentes, M.: The ERA-40 Archive, ERA-40 Project Report Series No. 17, ECMWF, Sept., 2004.

10 Lucarini, L. and Russell, G. L.: Comparison of mean climate trends in the northern hemisphere between National Centers for Environmental Prediction and two atmosphere-ocean model forced runs, *J. Geophys. Res.*, 107(D15), 4269, 2002.

Marti, O., Braconnot, P., Bellier, J., Benshila, R., Bony, S., Brockmann, P., Cadule, P., Caubel, A., Denvil, S., Dufresne, J.-L., Fairhead, L., Filiberti, M.-A., Foujols, M.-A., Fichetef, T.,  
15 Friedlingstein, P., Gosse, H., Grandpeix, J.-Y., Hourdin, F., Krinner, G., Lvy, C., Madec, G., Musat, I., de Noblet, N., Polcher, J., and Talandier, C.: The new IPSL climate system model: IPSL-CM4, Technical Report, Institut Pierre Simon Laplace des Sciences de l'Environnement Global, IPSL, Case 101, 4 place Jussieu, Paris, France, 84, 2005.

New, M., Hulme, M., and Jones, P.: Representing Twentieth-Century Space-Time Climate Variability, Part 1: Development of a 1961–90 Mean Monthly Terrestrial Climatology, *J. Climate*,  
20 12, 829–856, 1999.

New, M., Hulme, M., and Jones, P.: Representing Twentieth-Century Space-Time Climate Variability. Part II: Development of a 1901–96 Monthly Grids of Terrestrial Surface Climate, *J. Climate*, 13, 2217–2238, 2000.

25 Osborn, T. J.: Simulating the winter North Atlantic Oscillation: the roles of internal variability and greenhouse gas forcing, *Climate Dyn.*, 22, 605–623, 2004.

Priestley, C. H. B. and Taylor, R. J.: On the assessment of surface heat flux and evaporation using large-scale parameters, *Mon. Weather Rev.*, 106, 81–92, 1972.

Schmidt, G. A., Ruedy, R., Hansen, J. E., Aleinov, I., Bell, N., Bauer, M., Bauer, S., Cairns, B., Canuto, V., Cheng, Y., Del Genio, A., Faluvegi, G., Friend, A. D., Hall, T. M., Hu, Y.,  
30 Kelley, M., Kiang, N. Y., Koch, D., Lacis, A. A., Lerner, J., Lo, K. K., Miller, R. L., Nazarenko, L., Oinas, V., Perlwitz, Ja., Perlwitz, Ju., Rind, D., Romanou, A., Russell, G. L., Sato, Mki., Shindell, D. T., Stone, P. H., Sun, S., Tausnev, N., Thresher, D., and Yao, M.-S.: Present day

---

**Circulation biases  
and changes in  
global climate  
models**A. P. van Ulden and  
G. J. van Oldenborgh

---

Title Page

Abstract

Introduction

Conclusions

References

Tables

Figures

◀

▶

◀

▶

Back

Close

Full Screen / Esc

Print Version

Interactive Discussion

atmospheric simulations using GISS ModelE: Comparison to in-situ, satellite and reanalysis data, *J. Climate*, accepted, 2005.

Thorpe, R. P.: The impact of changes in atmospheric and land surface physics on the thermohaline circulation response to anthropogenic forcing in HadCM3 and HadCM2, *Clim. Dyn.*, 24, 449–456, 2005.

Turnpenny, J. R., Crossley, J. F., Hulme, M., and Osborne, T. J.: Air flow influences on local climate: comparison of a regional climate model with observations over the United Kingdom, *Clim. Res.*, 20, 189–202, 2002.

Van den Hurk, B., Hirschi, M., Lenderink, G., van Meijgaard, E., van Ulden, A. P., Rockel, B., Hagemann, S., Graham, P., Kjellström, E., and Jones, R.: Soil control on run-off response to climate change in regional climate model simulations, *J. Climate*, accepted, 2005.

Van Oldenborgh, G. J., and van Ulden, A. P.: On the relationship between global warming, local warming in the Netherlands and changes in circulation in the 20th century, *Int. J. Climatol.*, 23, 1711–1724, 2003.

Volodin, E. M. and Diansky, N. A.: El-Nino reproduction in coupled general circulation model of atmosphere and ocean, *Russian meteorology and hydrology*, vol. 12, 5–14, 2004.

Washington, W. M., Weatherly, J. W., Meehl, G. A., Semtner Jr., A. J., Bettge, T. W., Craig, A. P., Strand Jr., W. G., Arblaster, J., Wayland, V. B., James, R., and Zhang, Y.: Parallel climate model (PCM) control and transient simulations, *Climate Dyn.*, 16, 755–774, 2000.

Yu, Y., Zhang, X., and Guo, Y.: Global coupled ocean- atmosphere general circulation models in LASG/IAP, *Adv. Atmos. Sci.*, 21, 444–455, 2004.

Yukimoto, S. and Noda, A.: Improvements of the Meteorological Research Institute Global Ocean-atmosphere Coupled GCM (MRI-CGCM2) and its climate sensitivity, Technical Report 10, NIES, Japan, [www.mri-jma.go.jp/Dep/cl/cl4/publications/yukimoto\\_CGER2002.pdf](http://www.mri-jma.go.jp/Dep/cl/cl4/publications/yukimoto_CGER2002.pdf), 2002.

**Table 1.** Models included in this study.

Model name	Short name	Originating group(s)	Country	Atmospheric resolution	Reference
CCCMA-CGCM3.1	CCC3.1	CCCMA	Canada	T47,L31	Kim et al. (2002)
CNRM-CM3	CNRM3	Meteo-France/CNRM	France	T63,L45	Salas-M'elia et al. (2005)
CSIRO-Mk3.0	CSIRO3	CSIRO	Australia	T63,L18	Gordon et al. (2002)
ECHAM5/MPI-OM	ECHAM5	MPI	Germany	T63,L31	Jungclaus et al. (2005)
FGOALS-g1.0	FGOALS	LASG/IAP	China	T42,L26	Yu et al. (2004)
GFDL-CM2.0	GFDL2.0	GFDL	USA	2.5°×2°,L24	Delworth et al. (2005)
GFDL-CM2.1	GFDL2.1	GFDL	USA	2.5°×2°,L24	Delworth et al. (2005)
GISS-AOM	GISSao	NASA/GISS	USA	4°×3°,L12	Lucarini & Russell (2002)
GISS-EH	GISSeh	NASA/GISS	USA	5°×4°,L20	Schmidt et al. (2005)
GISS-ER	GISSer	NASA/GISS	USA	5°×4°,L20	Schmidt et al. (2005)
INM-CM3.0	INM3	INM	Russia	5°×4°,L21	Volodin and Diansky (2004)
IPSL-CM4	IPSL4	IPSL	France	3.75×2.5,L19	Marti et al. (2005)
MIROC3.2(hires)	MIROChi	CCSR/NIES/FRCGC	Japan	T106,L56	K-1 developers (2004)
MIROC3.2(medres)	MIROCM	CCSR/NIES/FRCGC	Japan	T42,L20	K-1 developers (2004)
MRI-CGCM2.3.2	MRI2.3.2	MRI	Japan	T42,L30	Yukimoto and Noda (2002)
NCAR-CCSM3	CCSM3	NCAR	USA	T85,L26	Collins et al. (submitted, 2005) <sup>1</sup>
NCAR-PCM	PCM1	NCAR	USA	T42,L18	Washington et al. (2000)
UKMO-HadCM3	HadCM3	UKMO	U.K.	3.75×2.5,L19	Gordon et al. (2000)
UKMO-HadGEM1	HadGEM	UKMO	U.K.	1.875×1.25,L38	Johns et al. (2004)

<sup>1</sup>– Collins, W. D., Bitz, C. M., Blackmon, M. I., Bonan, G. B., Bretherton, C. S., Carton, J. A., Chang, P., Doney, S. C., Hack, J. J., Henderson, T. B., Kiehl, J. T., Large, W. G., McKenna, D. S., Santer, B. D., and Smith, R. D.: The Community Climate System Model: CCSM3, J. Climate, submitted, 2005.

## Circulation biases and changes in global climate models

A. P. van Ulden and  
G. J. van Oldenborgh

Title Page

Abstract

Introduction

Conclusions

References

Tables

Figures

◀

▶

◀

▶

Back

Close

Full Screen / Esc

Print Version

Interactive Discussion

**Table 2.** Quality of simulated mean sea level pressure on global and regional scales.

	Globe stde hPa	Tropics stde hPa	S.Lat. stde hPa	N.Lat stde hPa	Europe stde hPa	Globe expl. fraction	Tropics expl. fraction	S.Lat. expl. fraction	N.Lat. expl. fraction	Europe expl. fraction
CCC3.1	4.1	1.6	6.1	3.2	1.9	0.83	0.84	0.75	0.51	0.80
CNRM3	7.6	1.5	10.1	3.3	3.4	0.45	0.85	0.31	0.49	0.51
CSIRO3	5.6	1.9	6.0	4.6	2.8	0.69	0.77	0.77	0.31	0.68
ECHAM5	2.7	1.6	3.4	2.5	1.7	0.93	0.84	0.93	0.70	0.83
GFDL2.0	3.9	1.6	4.5	3.9	2.7	0.85	0.85	0.86	0.32	0.59
GFDL2.1	3.0	1.8	3.2	2.9	2.4	0.91	0.81	0.93	0.63	0.75
GISSao	8.9	1.6	13.0	3.6	2.8	0.24	0.83	-0.05	0.47	0.68
GISSeh	8.7	2.6	11.6	4.7	3.9	0.27	0.58	0.18	-0.09	0.16
GISSer	8.1	2.6	10.4	5.4	4.5	0.36	0.60	0.35	-0.34	-0.14
FGOALS	4.5	1.8	5.5	4.2	3.5	0.80	0.80	0.80	0.18	0.43
INM3	4.1	1.8	4.8	4.0	3.6	0.83	0.80	0.85	0.30	0.42
IPSL4	12.6	1.8	19.1	5.5	3.2	-0.56	0.79	-1.36	-0.23	0.53
MIROChi	4.6	1.6	5.2	2.9	1.7	0.79	0.83	0.83	0.68	0.85
MIROCm	4.5	1.9	5.8	3.5	2.6	0.80	0.78	0.78	0.56	0.71
MRI2.3.2	4.3	1.5	5.1	4.3	2.4	0.82	0.86	0.84	0.30	0.75
CCSM3	5.4	1.8	5.2	5.0	5.3	0.71	0.80	0.82	-0.23	-0.60
PCM	6.4	2.8	9.7	3.8	4.8	0.60	0.50	0.43	0.34	-0.08
HadCM3	4.6	2.1	4.7	4.4	2.5	0.79	0.72	0.86	0.23	0.69
HadGEM	4.0	2.1	5.3	2.8	1.9	0.84	0.73	0.82	0.64	0.83

## Circulation biases and changes in global climate models

A. P. van Ulden and  
G. J. van Oldenborgh

Title Page

Abstract

Introduction

Conclusions

References

Tables

Figures

◀

▶

◀

▶

Back

Close

Full Screen / Esc

Print Version

Interactive Discussion

**Circulation biases and changes in global climate models**

A. P. van Ulden and G. J. van Oldenborgh

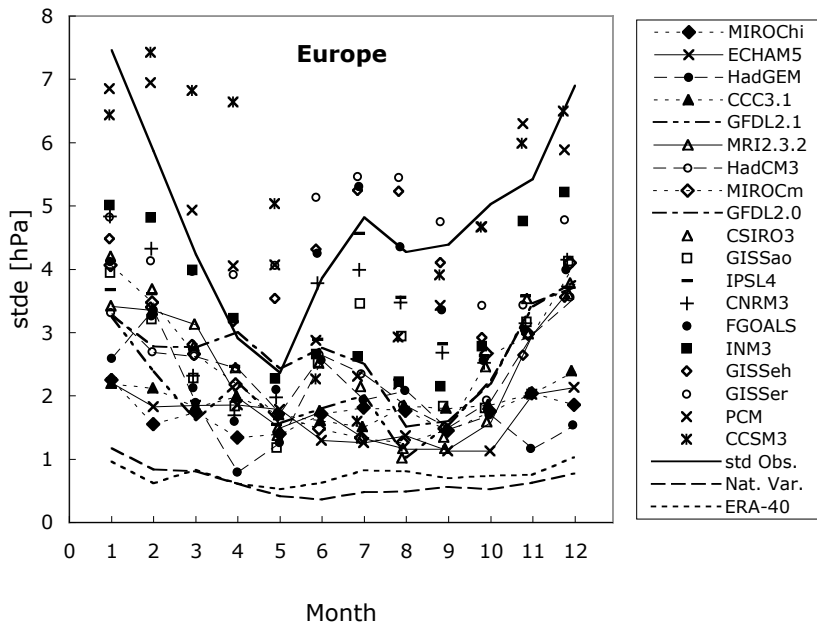


**Fig. 1.** Spatial standard deviation of the difference between simulated sea level pressure fields and the longterm mean observed pressure field. Std Obs. is the spatial standard deviation of the observed field. Nat. Var. is the mean spatial standard deviation of the differences between 30 year averaged observed fields and the longterm mean observed field. ERA-40 is the spatial standard deviation of ERA-40 averaged over the last 30 year, relative to the long-term mean observed field.

Title Page

Abstract

Introduction

Conclusions

References

Tables

Figures

◀

▶

◀

▶

Back

Close

Full Screen / Esc

Print Version

Interactive Discussion

---

**Circulation biases  
and changes in  
global climate  
models**A. P. van Ulden and  
G. J. van Oldenborgh

---

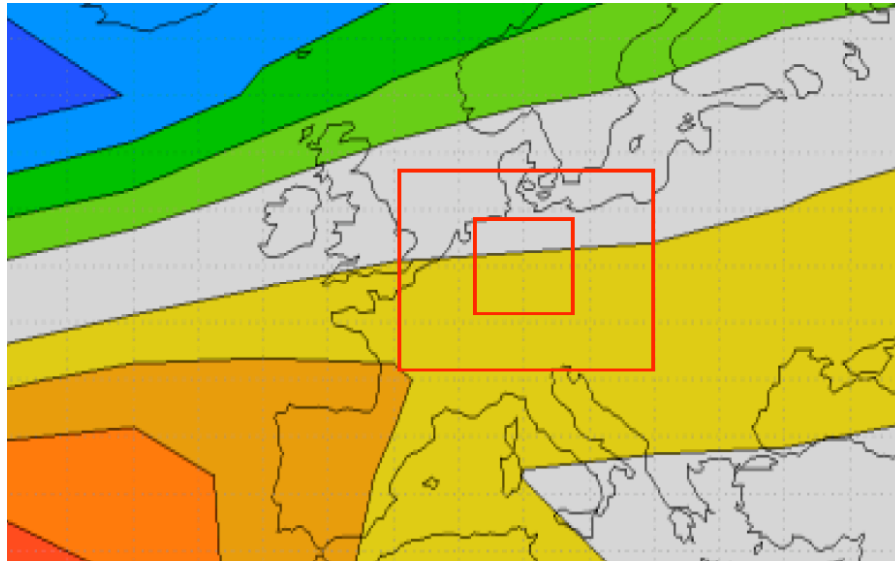
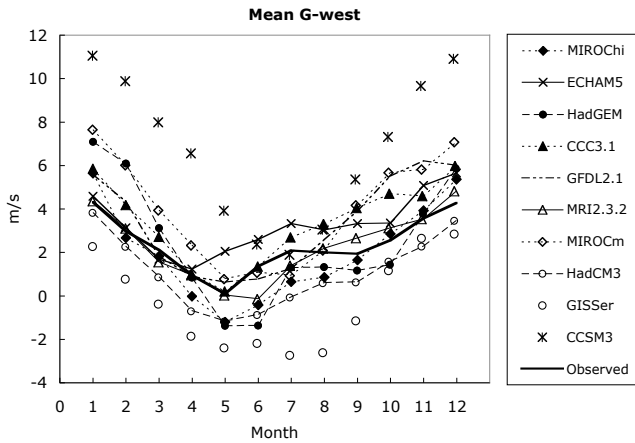


**Fig. 2.** European domains. The full picture gives the European test domain for pressure patterns used in Sect. 2. It depicts the annual mean observed sea level pressure field for the 20th century. The interval width is 2 hPa, except for the grey region, which represents the interval 1012–1016 hPa. In the southwest corner the Azores High is visible, while in the northwest the Iceland Low can be seen. The large rectangle is the region West–Central Europe for which the geostrophic flow indices are computed. The small rectangle is the test region for temperature and precipitation.

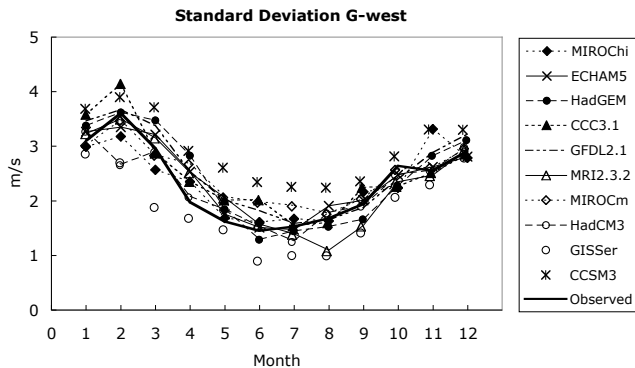
[Title Page](#)[Abstract](#)[Introduction](#)[Conclusions](#)[References](#)[Tables](#)[Figures](#)[◀](#)[▶](#)[◀](#)[▶](#)[Back](#)[Close](#)[Full Screen / Esc](#)[Print Version](#)[Interactive Discussion](#)

**Circulation biases and changes in global climate models**

A. P. van Ulden and G. J. van Oldenborgh



(a)



(b)

**Fig. 3.** (a) Mean west component of the geostrophic wind for the 20th century. (b) Standard deviation of west component of geostrophic wind.

Title Page

Abstract

Introduction

Conclusions

References

Tables

Figures

◀

▶

◀

▶

Back

Close

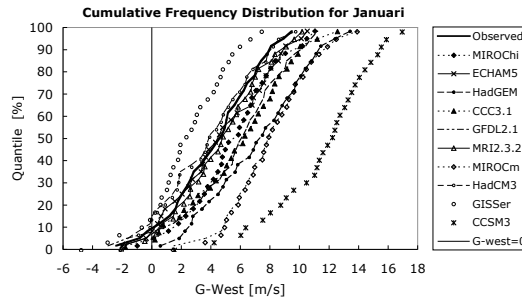
Full Screen / Esc

Print Version

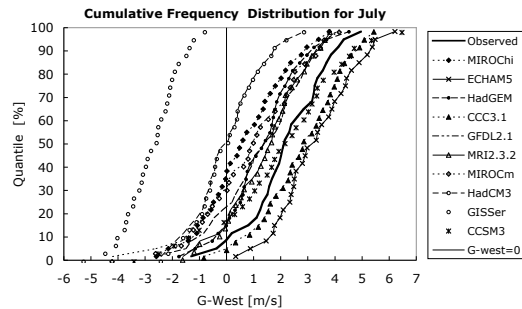
Interactive Discussion

Circulation biases and changes in global climate models

A. P. van Ulden and G. J. van Oldenborgh



(a)



(b)

Fig. 4. (a) Cumulative frequency distribution of the west component of the geostrophic wind for January in the 20th century. (b) As Fig. 4a, but for July.

Title Page

Abstract

Introduction

Conclusions

References

Tables

Figures

◀

▶

◀

▶

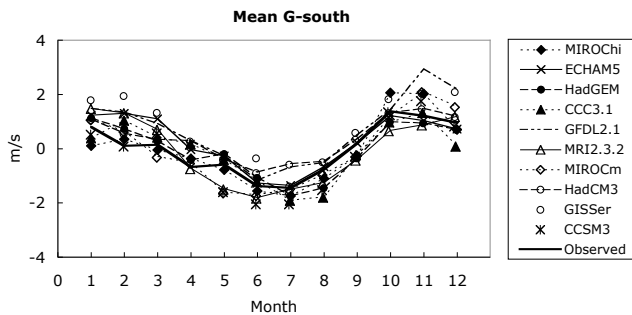
Back

Close

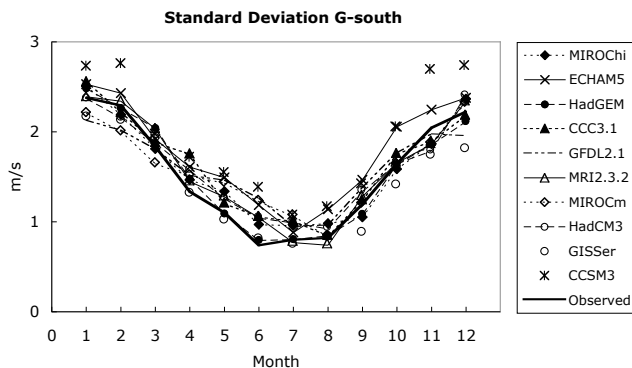
Full Screen / Esc

Print Version

Interactive Discussion

**Circulation biases  
and changes in  
global climate  
models**A. P. van Ulden and  
G. J. van Oldenborgh

(a)



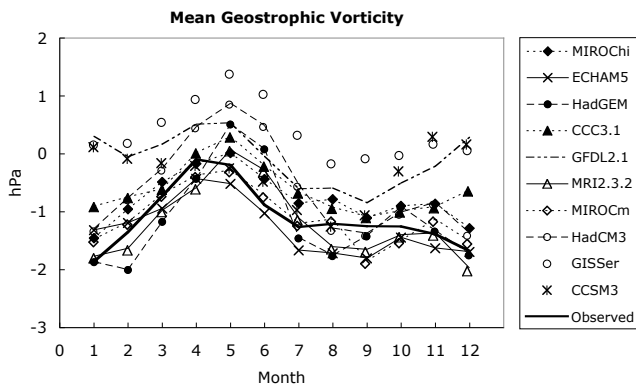
(b)

**Fig. 5.** (a) Mean south component of the geostrophic wind for the 20th century. (b) Standard deviation of south component of geostrophic wind.

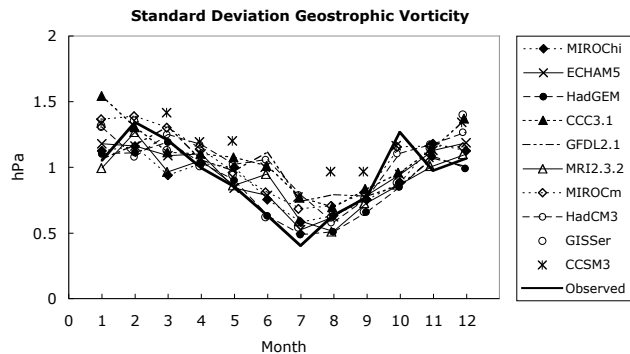
[Title Page](#)[Abstract](#)[Introduction](#)[Conclusions](#)[References](#)[Tables](#)[Figures](#)[◀](#)[▶](#)[◀](#)[▶](#)[Back](#)[Close](#)[Full Screen / Esc](#)[Print Version](#)[Interactive Discussion](#)

**Circulation biases and changes in global climate models**

A. P. van Ulden and G. J. van Oldenborgh



(a)



(b)

**Fig. 6. (a)** Mean geostrophic vorticity for the 20th century. **(b)** Standard deviation of geostrophic vorticity for the 20th century.

Title Page

Abstract

Introduction

Conclusions

References

Tables

Figures

◀

▶

◀

▶

Back

Close

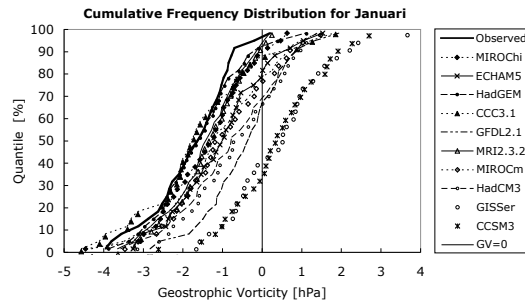
Full Screen / Esc

Print Version

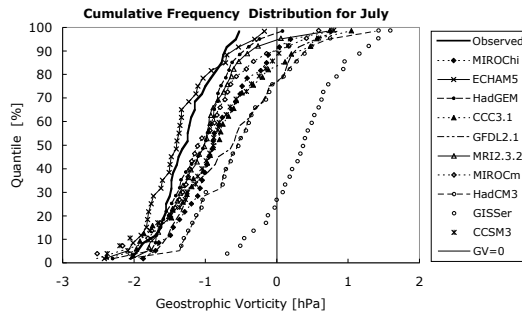
Interactive Discussion

## Circulation biases and changes in global climate models

A. P. van Ulden and  
G. J. van Oldenborgh



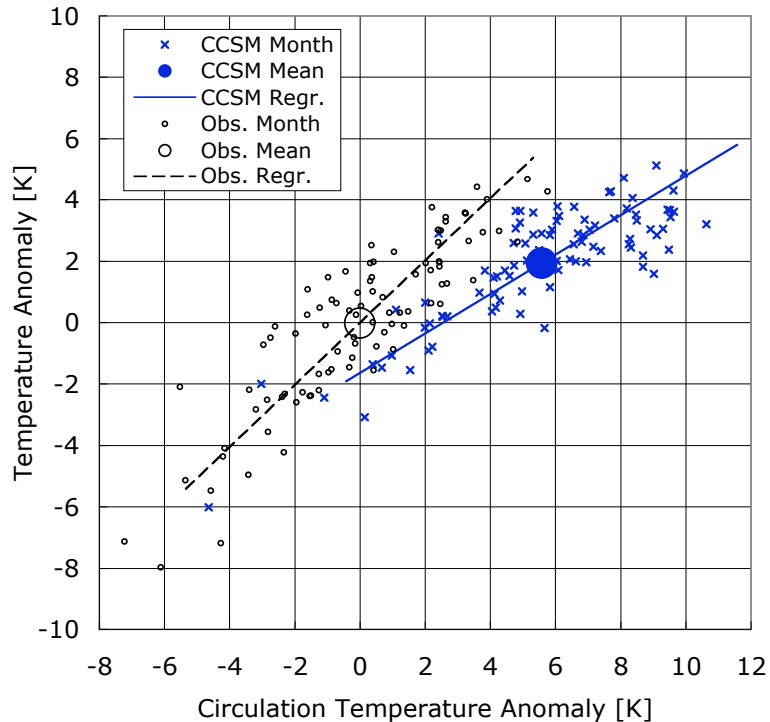
(a)



(b)

**Fig. 7.** (a) Cumulative frequency distribution of the geostrophic vorticity in the 20th century for January. (b) Cumulative frequency distribution of the geostrophic vorticity in the 20th century for July.

[Title Page](#)
[Abstract](#)
[Introduction](#)
[Conclusions](#)
[References](#)
[Tables](#)
[Figures](#)
[◀](#)
[▶](#)
[◀](#)
[▶](#)
[Back](#)
[Close](#)
[Full Screen / Esc](#)
[Print Version](#)
[Interactive Discussion](#)

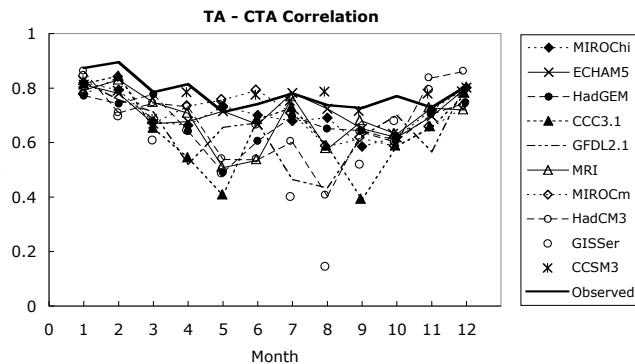
**Circulation biases  
and changes in  
global climate  
models**A. P. van Ulden and  
G. J. van Oldenborgh

**Fig. 8.** Scatter plots of observed and simulated (CCSM3.2) July temperature anomalies (TA) against circulation temperature anomalies (CTA) for the 20th century. Shown are monthly anomalies, 20th century mean anomalies and regression lines. The length of the regression lines is 4 standard deviations for both axes. The correlations between TA and CTA are 0.87 for the observations and 0.84 for the model simulations. The model simulations have a warm temperature bias of 1.9 K and a warm circulation temperature bias of 5.6 K. The slope of the regression line is 0.64. This produces a temperature bias due to the circulation bias of 3.6 K. This indicates that the model would have shown a negative residual temperature bias of  $-1.7$  K, if it had simulated no mean circulation bias.

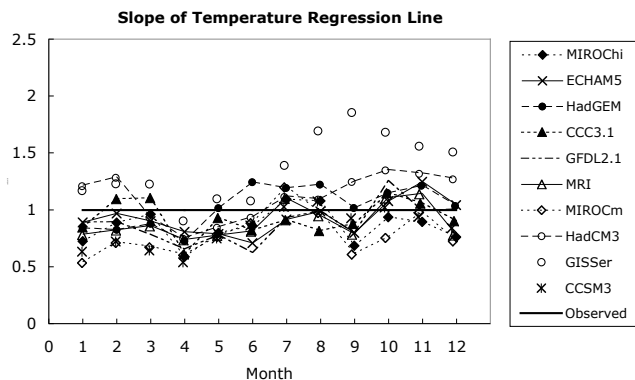
[Title Page](#)[Abstract](#)[Introduction](#)[Conclusions](#)[References](#)[Tables](#)[Figures](#)[◀](#)[▶](#)[◀](#)[▶](#)[Back](#)[Close](#)[Full Screen / Esc](#)[Print Version](#)[Interactive Discussion](#)

**Circulation biases  
and changes in  
global climate  
models**

A. P. van Ulden and  
G. J. van Oldenborgh



(a)



(b)

**Fig. 9.** (a) TA–CTA correlations for the 20th century. (b) Slope  $S_T = \Sigma TA / \Sigma CTA$ .

Title Page

Abstract

Introduction

Conclusions

References

Tables

Figures

◀

▶

◀

▶

Back

Close

Full Screen / Esc

Print Version

Interactive Discussion

**Circulation biases and changes in global climate models**

A. P. van Ulden and G. J. van Oldenborgh

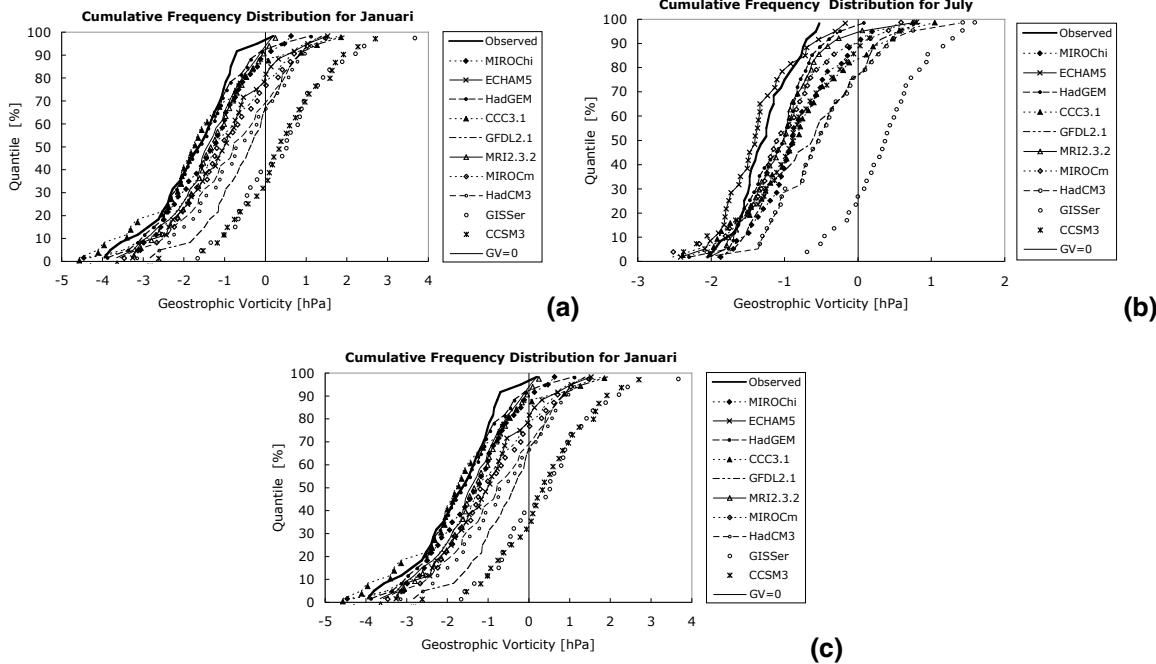


**Fig. 10.** Temperature bias for 20th century. **(a)** Total, **(b)** Circulation, **(c)** Residual.

Title Page

Abstract

Introduction

Conclusions

References

Tables

Figures

◀

▶

◀

▶

Back

Close

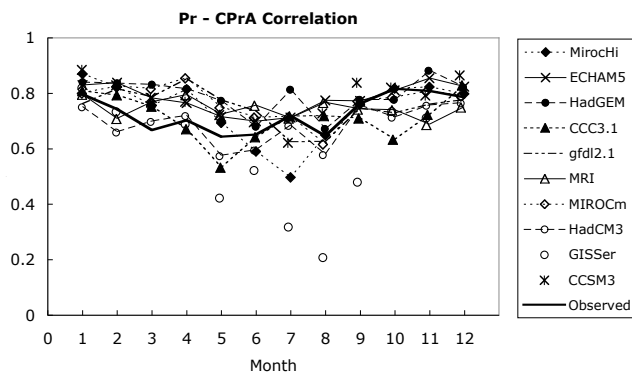
Full Screen / Esc

Print Version

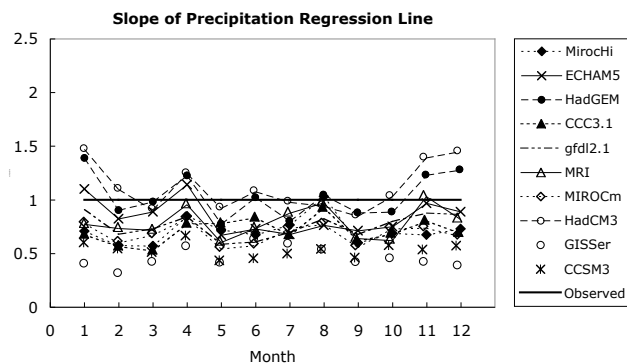
Interactive Discussion

## Circulation biases and changes in global climate models

A. P. van Ulden and  
G. J. van Oldenborgh



(a)



(b)

**Fig. 11.** (a) Correlations between precipitation and circulation for the 20th century. (b) Slope:  $S_{Pr} = \Sigma_{Pr} / \Sigma_{CPrA}$  for the 20th century.

[Title Page](#)
[Abstract](#)
[Introduction](#)
[Conclusions](#)
[References](#)
[Tables](#)
[Figures](#)
[◀](#)
[▶](#)
[◀](#)
[▶](#)
[Back](#)
[Close](#)
[Full Screen / Esc](#)
[Print Version](#)
[Interactive Discussion](#)

**Circulation biases and changes in global climate models**

A. P. van Ulden and G. J. van Oldenborgh

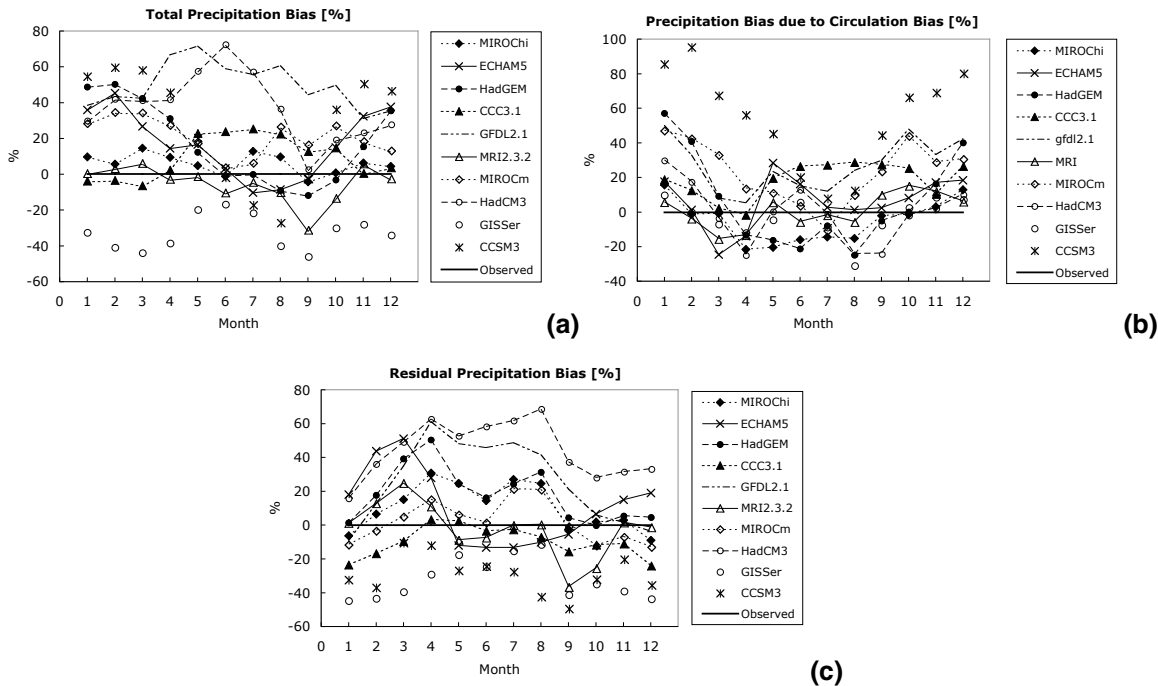


**Fig. 12.** Precipitation bias for 20th century. **(a)** Total, **(b)** Circulation, **(c)** Residual.

Title Page

Abstract Introduction

Conclusions References

Tables Figures

◀ ▶

◀ ▶

Back Close

Full Screen / Esc

Print Version

Interactive Discussion

**Circulation biases and changes in global climate models**

A. P. van Ulden and G. J. van Oldenborgh

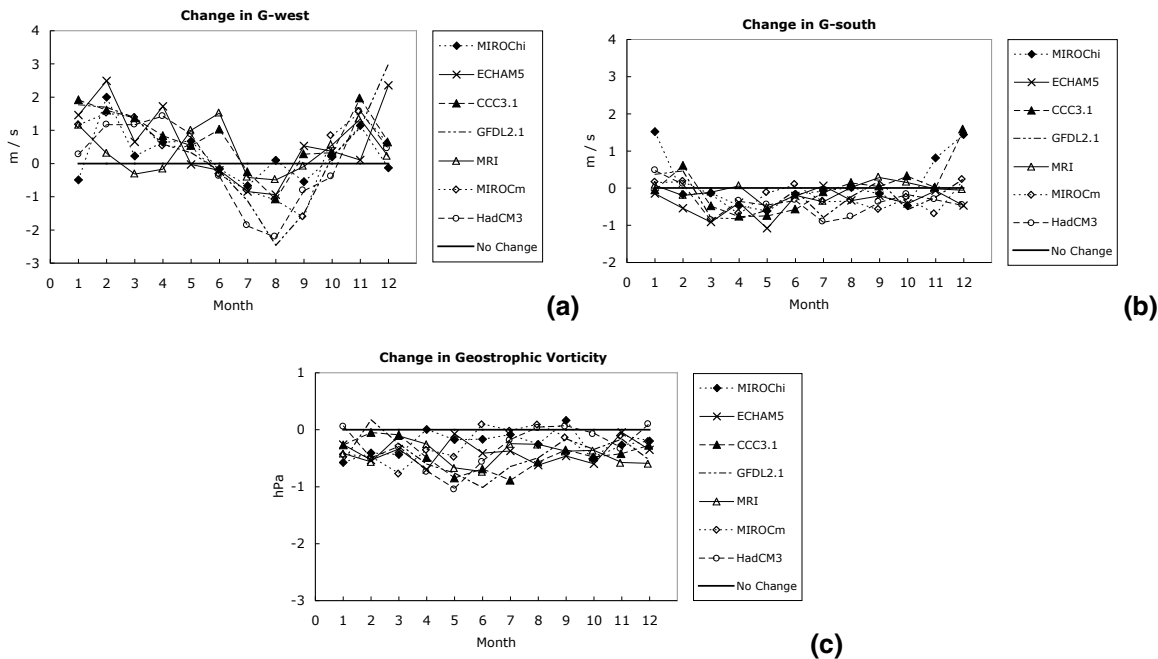


**Fig. 13.** Circulation changes from 20th century to 2071–2100.

Title Page

Abstract Introduction

Conclusions References

Tables Figures

◀ ▶

◀ ▶

Back Close

Full Screen / Esc

Print Version

Interactive Discussion

**Circulation biases  
and changes in  
global climate  
models**

A. P. van Ulden and  
G. J. van Oldenborgh

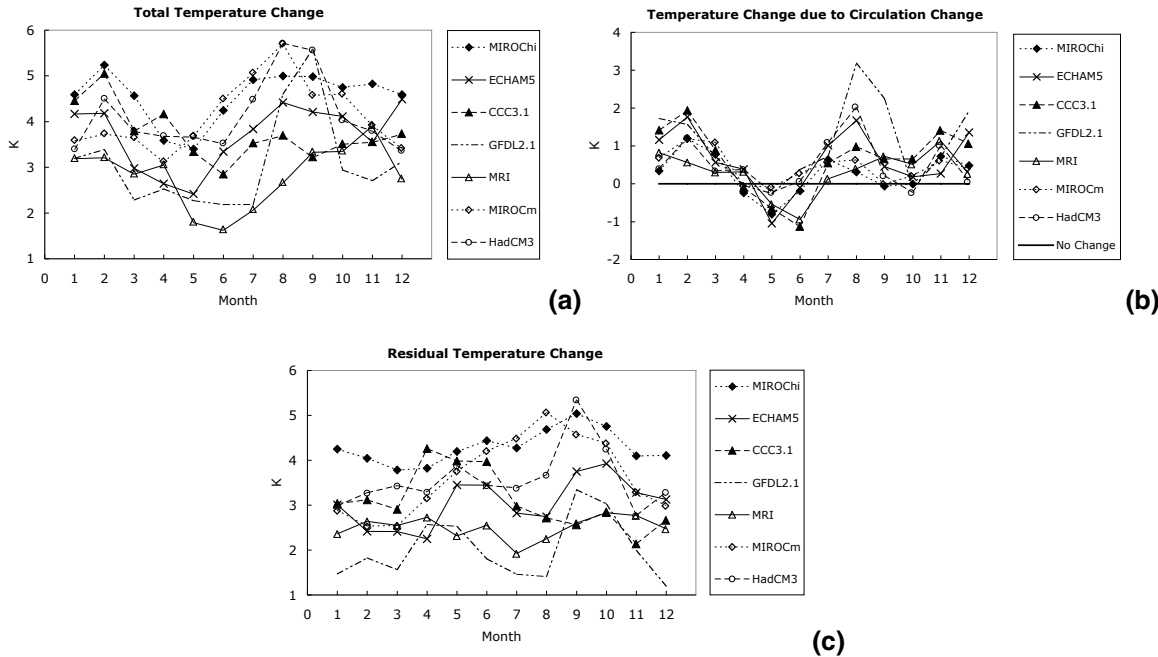


**Fig. 14.** Temperature changes from 20th century to 2071–2100. **(a)** Total, **(b)** Circulation, **(c)** Residual.

Title Page

Abstract

Introduction

Conclusions

References

Tables

Figures

◀

▶

◀

▶

Back

Close

Full Screen / Esc

Print Version

Interactive Discussion

Circulation biases and changes in global climate models

A. P. van Ulden and G. J. van Oldenborgh

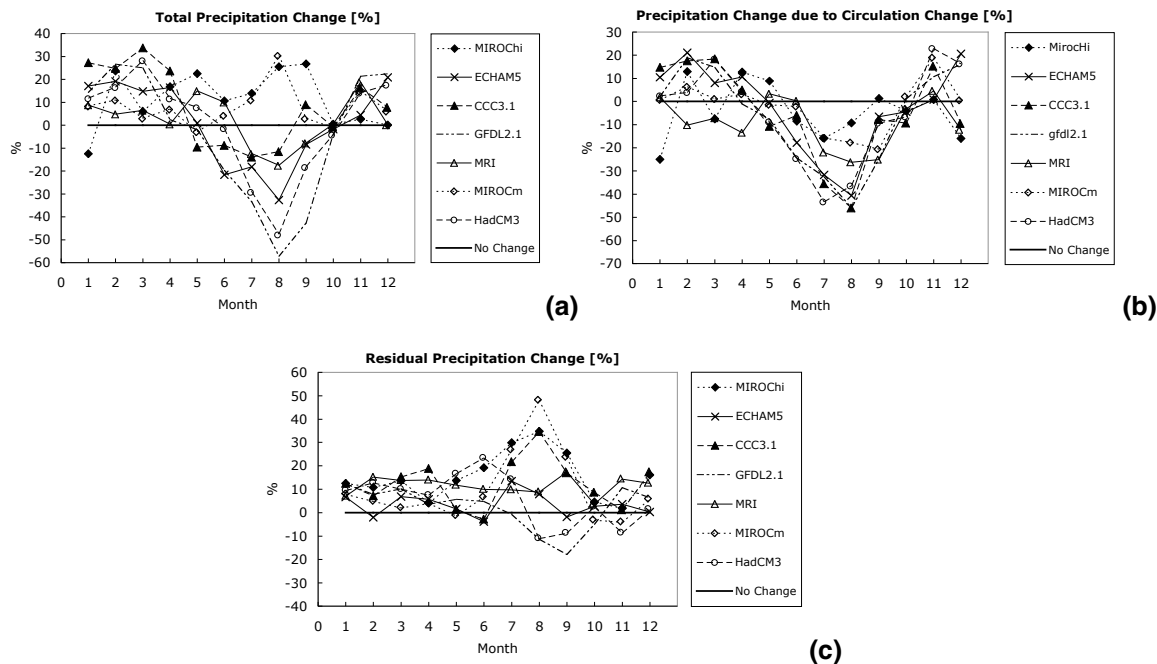


Fig. 15. Precipitation changes from 20th century to 2071–2100. (a) Total, (b) Circulation, (c) Residual.

Title Page

Abstract Introduction

Conclusions References

Tables Figures

◀ ▶

◀ ▶

Back Close

Full Screen / Esc

Print Version

Interactive Discussion

## Circulation biases and changes in global climate models

A. P. van Ulden and  
G. J. van Oldenborgh

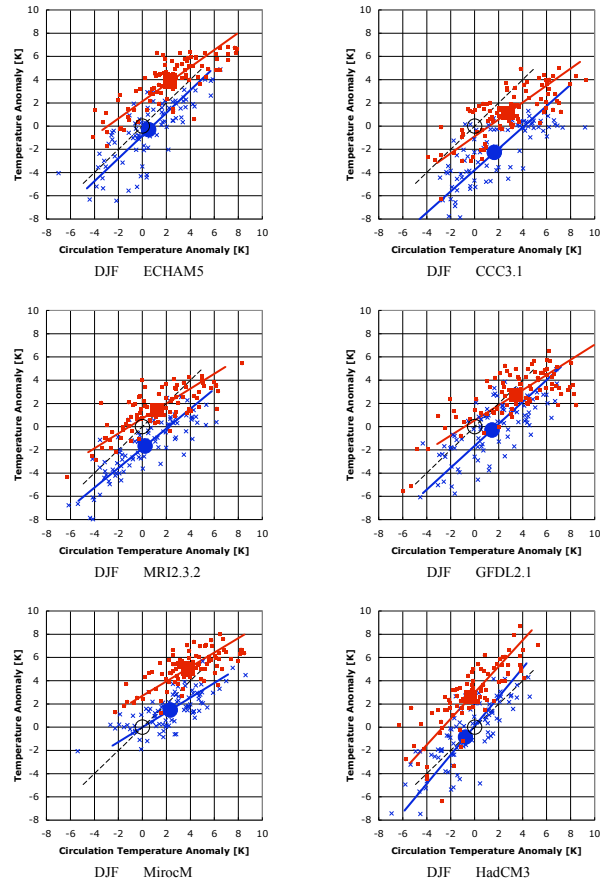


**Fig. 16.** Temperature-Circulation for winter months. Black: Observed; open circle: mean, broken line: regression, blue: simulated 1971–2000; solid circle: mean, line: regression, crosses: monthly values, red: 2071–2100; solid square: mean, solid line: regression, small squares: monthly values. The length of the regression lines is 4 standard deviations for both axes.

[Title Page](#)
[Abstract](#)
[Introduction](#)
[Conclusions](#)
[References](#)
[Tables](#)
[Figures](#)
[◀](#)
[▶](#)
[◀](#)
[▶](#)
[Back](#)
[Close](#)
[Full Screen / Esc](#)
[Print Version](#)
[Interactive Discussion](#)

**Circulation biases and changes in global climate models**

A. P. van Ulden and G. J. van Oldenborgh

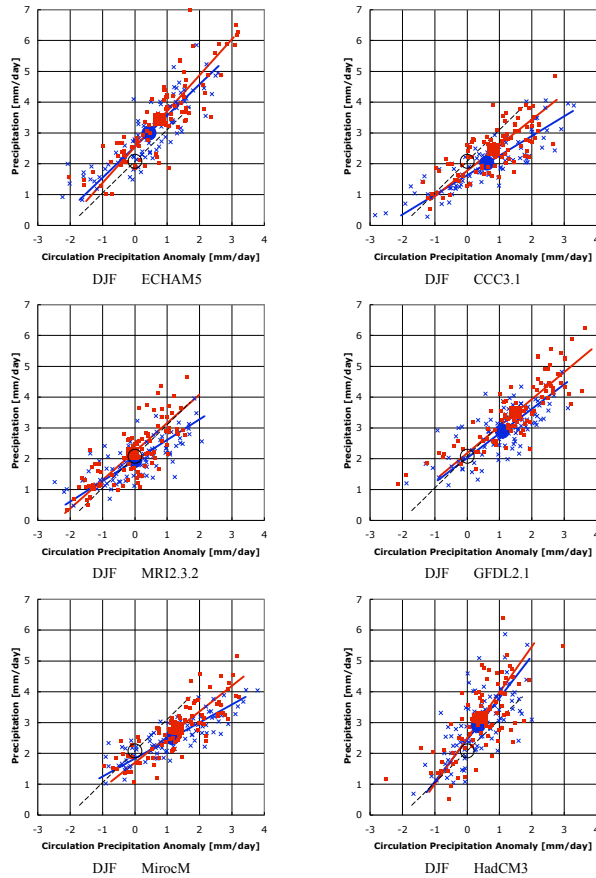


Fig. 17. As Fig. 16, but for precipitation.

Title Page

Abstract

Introduction

Conclusions

References

Tables

Figures

◀

▶

◀

▶

Back

Close

Full Screen / Esc

Print Version

Interactive Discussion

**Circulation biases and changes in global climate models**

A. P. van Ulden and G. J. van Oldenborgh

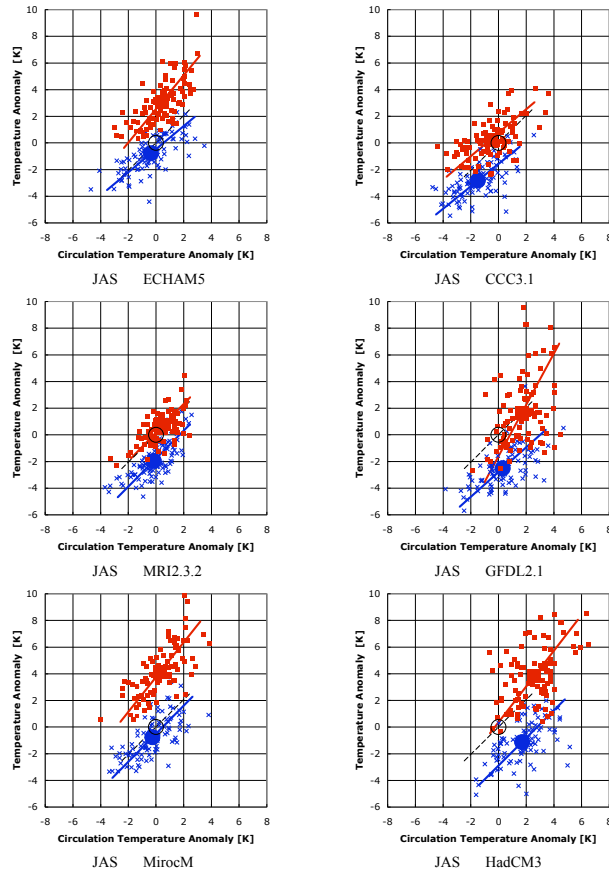


Fig. 18. As Fig. 16, but for late summer months.

Title Page

Abstract

Introduction

Conclusions

References

Tables

Figures

◀

▶

◀

▶

Back

Close

Full Screen / Esc

Print Version

Interactive Discussion

**Circulation biases  
and changes in  
global climate  
models**

A. P. van Ulden and  
G. J. van Oldenborgh

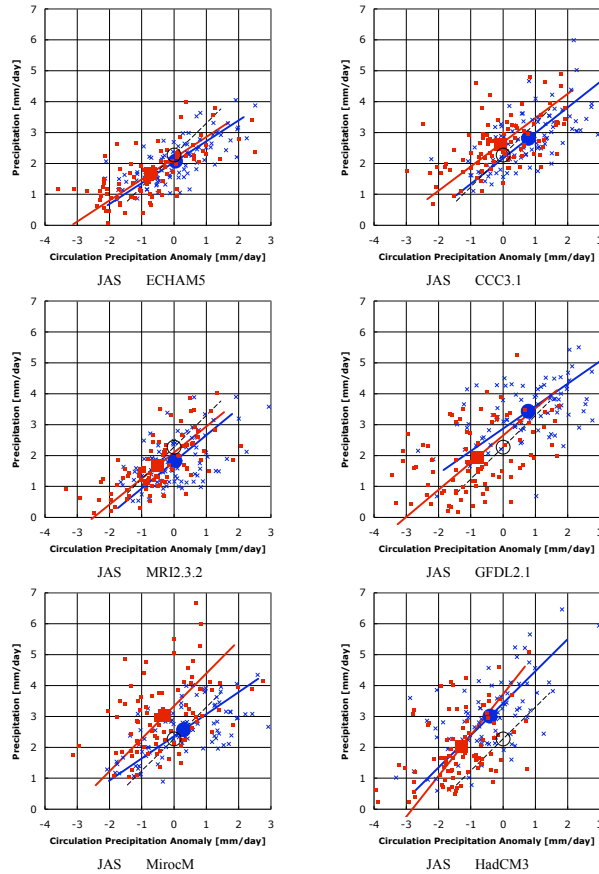


Fig. 19. As Fig. 17, but for late summer months.

Title Page

Abstract

Introduction

Conclusions

References

Tables

Figures

◀

▶

◀

▶

Back

Close

Full Screen / Esc

Print Version

Interactive Discussion